

Cite this: *Nanoscale Adv.*, 2021, 3, 3167

Machine learning methods for multi-walled carbon nanotubes (MWCNT) genotoxicity prediction†

Marianna Kotzabasaki,  ‡*, Iason Sotiropoulos,  ‡, Costas Charitidis 
and Haralambos Sarimveis  *

Multi-walled carbon nanotubes (MWCNTs) are made of multiple single-walled carbon nanotubes (SWCNTs) which are nested inside one another forming concentric cylinders. These nanomaterials are widely used in industrial and biomedical applications, due to their unique physicochemical characteristics. However, previous studies have shown that exposure to MWCNTs may lead to toxicity and some of the physicochemical properties of MWCNTs can influence their toxicological profiles. *In silico* modelling can be applied as a faster and less costly alternative to experimental (*in vivo* and *in vitro*) testing for the hazard characterization of MWCNTs. This study aims at developing a fully validated predictive nanoinformatics model based on statistical and machine learning approaches for the accurate prediction of genotoxicity of different types of MWCNTs. Towards this goal, a number of different computational workflows were designed, combining unsupervised (Principal Component Analysis, PCA) and supervised classification techniques (Support Vectors Machine, "SVM", Random Forest, "RF", Logistic Regression, "LR" and Naïve Bayes, "NB") and Bayesian optimization. The Recursive Feature Elimination (RFE) method was applied for selecting the most important variables. An RF model using only three features was selected as the most efficient for predicting the genotoxicity of MWCNTs, exhibiting 80% accuracy on external validation and high classification probabilities. The most informative features selected by the model were "Length", "Zeta average" and "Purity".

Received 22nd July 2020
Accepted 11th April 2021

DOI: 10.1039/d0na00600a

rsc.li/nanoscale-advances

Introduction

Multi-walled carbon nanotubes (MWCNTs) are long, hollow cylindrical tubes with outer diameters in the range 3–30 nm and lengths that can reach the order of cm. MWCNTs have large length-to-diameter ratio, varying between 10 and ten million, while their wall thickness is quite constant along the axis, thus the inner channel is straight.¹

MWCNTs were discovered by Sumio Iijima in 1991,² as soot-like products in the Krätschmer-Huffman arc discharge synthesis reactor used for the formation of fullerene (C₆₀).³ Later, single-walled carbon nanotubes (SWCNTs) were discovered.⁴ SWCNTs are assembled into coaxial Russian-doll structures, forming MWCNTs with walls corresponding to each single-walled nanotube. The intertubular distance in MWCNTs is 0.340 nm. The main difference between SWCNTs and MWCNTs is that the former are flexible, while the latter are tough and rigid, rod-shaped structures. SWCNTs are also of

smaller widths, with diameters typically in the range 1–2 nm, with curved structures rather than straight.⁵

Due to unique tubular structures and perfect covalent C–C bonding, MWCNTs exhibit fascinating physical and chemical properties, such as ultra-high mechanical strength, very good electrical and thermal conductivity ($\sim 3000 \text{ W m}^{-1} \text{ K}^{-1}$, comparable to diamond), large aspect ratios, high surface area (SA), desirable chemical and environmental stability and distinct optical characteristics.⁶ MWCNTs are the strongest materials ever discovered. A MWCNT's highest measured tensile strength was up to 63 GPa, which is around 50 times higher than steel.^{5,7}

The aforementioned MWCNTs' superb (and unique) characteristics give them great potential in various emerging applications in areas from biotechnology (imaging, tissue engineering, sensors and targeted drug delivery) to electronics (energy production and storage, transistors) and other fields of materials science (photonics, multi-functional coatings/films and nanocomposites).⁸ In the biomedical area, a number of applications of MWCNTs have been proposed including drug delivery, diagnosis and imaging, cancer diagnosis, gene therapy, photothermal therapy, *etc.* For instance, MWCNTs are efficiently used as carrier to deliver quantum dots (QDs) and proteins into cancer cells because QDs have photoluminescent properties, which are beneficial in bioimaging. MWCNTs may

School of Chemical Engineering, National Technical University of Athens, 9 Heroon Polytechniou Street, Zografou Campus, 15780, Athens, Greece. E-mail: mariannako@chemeng.ntua.gr; hsarimv@central.ntua.gr; Fax: +30 2107723138; Tel: +30 2107723236; +302107723237

† Electronic supplementary information (ESI) available. See DOI: 10.1039/d0na00600a

‡ Both authors contributed equally to this work.

also be used for the treatment of HIV/AIDS and Neurodegenerative Diseases like Alzheimer Syndrome, while carboxylated-nanotubes may have potential as antioxidants in anti-ageing cosmetics and food preservation. Moreover, they have emerged as potential biosensors and nanorobots in diagnostics and as nanoprobes in scanning probe microscopy.⁹

Although MWCNTs have exceptional physicochemical properties, concerns have been raised about their safety, which are due to their small sizes and fibrous structures. MWCNTs may pose hazards, similar to asbestos.¹⁰ A number of physicochemical properties and characteristics of MWCNTs have been associated with their toxicological profiles: tube length and diameter, specific surface area, surface reactivity, metal impurities/catalysts, agglomeration state/dispersion, surface functionalization and rigidity/flexibility.¹¹ As Poland *et al.* reported,¹² longer MWCNTs exhibited stronger inflammation activity to mouse in the intraperitoneal administration route. Lam *et al.*,¹³ also pointed out that the content of metal used as a catalyst is very important. They concluded that the impure metals may enhance the pulmonary toxicity of carbon nanoforms. In other studies, it has been shown that contamination of amorphous carbon in the MWCNTs may affect strongly their biological activity, compared to purer MWCNTs.^{14,15} Additionally, it was reported that the agglomeration state of carbon nanomaterials also affected toxicity. Exposure to well-dispersed MWCNTs led to fewer granulomatous lesions in the lung, while non-dispersed nanostructures produced granulomatous inflammation.⁹

The investigation and study of potential hazards resulting from exposure to engineered MWCNTs is of particular interest in the nanotoxicology area. *In silico* predictive modelling is a computational data-driven approach that can be applied for the prediction of adverse effects of MWCNTs, in the effort to reduce animal testing. This aligns with Annex XI¹⁶ of Registration, Evaluation, Authorisation and Restriction of Chemicals (REACH) regulation (European Parliament and Council 2006), which describes alternative (non-animal) approaches such as grouping and read-across,¹⁷ Quantitative Structure–Activity Relationship (QSAR),¹⁸ *in vitro* methods and weight of evidence, which can be used instead of *in vivo* tests to examine and evaluate the risks of exposure to chemicals.

Read-across methods are based on the hypothesis that similar chemical substances, follow a regular pattern, based on their chemical composition and/or physicochemical (PC) properties and may also have comparable toxicological properties. Thus, the toxicological profile of one target substance can be predicted by using data for the same endpoint from other reference substances. Grouping of MWCNTs types to read-across data for toxicological endpoints has been efficiently evaluated by Aschberger *et al.*,¹¹ following the workflow proposed by the European Chemical Agency (ECHA) for grouping and reading across nanomaterials.¹⁹

Nano-QSARs, are mathematical models, which are based on the idea that the structure of a substance affects its activity and thus similar structures exhibit similar activities. Molecular descriptors (which are the physicochemical properties of MWCNTs in our case) play a fundamental role in QSAR and

other *in silico* models, since they formally are the numerical representation of a molecular structure. For instance, Kotzabasaki *et al.*²⁰ developed a robust QSAR model for predicting the nanotoxicity of superparamagnetic iron oxide nanoparticles (SPIONs) in stem-cell monitoring applications, using as molecular descriptors only the “overall particle size” and the “magnetic core chemical composition” of SPIONs. Kim²¹ and co-workers have successfully proposed a nano-QSAR model based on Quasi-SMILES to predict the cytotoxicity of MWCNTs to human lung cells.

In this study, we have developed a fully validated QSAR model for the prediction of genotoxicity of MWCNTs. Firstly, we selected 15 different types of MWCNTs and constructed a dataset that includes both physicochemical and toxicological data. Genotoxicity was selected as the hazard endpoint. According to REACH, genotoxicity testing is required, even at the lowest tonnage level (above 1 tonne per year per manufacturer/importer) for all substances manufactured in the EU.²² Next, we developed and fully validated a nanotoxicity classification QSAR model for predicting genotoxicity of MWCNTs using physicochemical characteristics as input features. A number of cheminformatics workflows based on machine learning algorithms, were constructed and implemented in order to produce the best performing model. The modelling workflows were designed to include the selection of the most important variables affecting the toxicity of MWCNTs and the definition of the domain of applicability (DOA)²³ of the predictive model. The model was finally implemented as a ready-to-use web application in the Jaqpot computational platform (<https://app.jaqpot.org/>) and is available to the community through the BIORIMA virtual organisation.

Computational methodology

Predictive modeling workflow

This particular case study follows a workflow shown below in algorithm of Fig. 1.

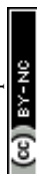
Step 1. The *Data collection* step consisted of a systematic search through the literature for collecting physicochemical properties and information about genotoxicity of MWCNTs and organizing the data in a ready for modelling dataset, containing 15 analogues and 34 features.

Step 2. During the *Data Pre-processing* step, we performed gap filling, data scaling and data reduction *via* the Principal Component Analysis (PCA)²⁴ algorithm.

Step 3. In the *Train–Test Split* step, the dataset was partitioned into two subsets. 10 analogues were used for training the models and the remaining analogues were used as external validation set to test the model performances.

Step 4. During the *Model Optimization and Train* step the hyperparameters of each model were optimized and a number of predictive nano-QSAR models were developed.

Step 5. The *Performance Test* step was used for testing the performance of the models using various statistical metrics, including the accuracy score and the Matthews correlation coefficient (MCC) and validating the robustness by calculating cross validation²⁵ scores.



Algorithm 1. Predictive Modelling Workflow**Step 1. Data Collection**

- Literature Research
- Dataset construction

Step 2. Data Pre-Processing

- Filling gaps
- Data scaling
- Unsupervised Learning

Step 3. Train – Test Split

- Split the dataset into one for training the model and one for testing it, using the Kennard-Stone algorithm

for model in Supervised Techniques do**Step 4. Model Optimization and Train**

- Calculation of the optimum hyperparameters
- Training of the model

Step 5. Performance Test

- Calculation of performance testing metrics such as the accuracy score and the Matthews correlation coefficient Robustness testing

Step 6. Feature Selection

- Selection of features with the highest predictive performance

end for

Step 7. Select the best performing model

- Define the Domain of Applicability
- Deploy the model on Jaqpot

Fig. 1 Workflow of data collection, pre-processing, model development, validation and analysis.

Step 6. In the *Feature Selection* step, the features with the higher predictive importance were selected and steps 4 and 5 were repeated using only the selected features as input information.

In the final step of this study, the model with the best performance was chosen and was implemented as a user-friendly web application in the Jaqpot platform.

Data collection and treatment

Fifteen high purity MWCNTs were selected, based on the richness and quality of the available physicochemical and toxicological data. Information on these MWCNTs was gathered from relevant MWCNT dossiers and from peer reviewed literature.^{11,26–29} According to previous studies, ten out of the fifteen MWCNTs (NRCWE040s – NRCWE-049)^{28,29} can be organized into three groups with respect to their physicochemical properties (thin, thick and short, group I–III, respectively). Each group included three functionalized MWCNTs which differed in the type of functionalization: a pristine, an –OH and a –COOH type. Group III also included a –NH₂ type functionalized MWCNT.²⁷ The five remaining analogues were taken from the

Table 1 The characteristics (features) of MWCNTs used in QSAR modelling

Features
Carbon purity (%) ¹¹
Minimum length (nm) ²⁹
Maximum length (nm) ²⁹
Average length (nm) ²⁹
Minimum diameter (nm) ²⁹
Maximum diameter (nm) ²⁹
Average diameter (nm) ²⁹
Specific surface area (SSA) measured by BET (m ² g ^{−1}) ²⁹
% Impurities (Fe ₂ O ₃ , CoO, NiO, MgO, MnO) ²⁹
Concentration of endotoxins (Eu ml ^{−1}) ²⁹
Combustion elemental analysis (CEA), C, H, N, O (wt%) ²⁷
Surface coatings OH, COOH, NH ₂ , (mmol g ^{−1}) ²⁷
Zeta average (Z _{ave}) batch and zeta average at 12.5 and 200 µg ml ^{−1} (nm) ²⁷
Polydispersity index (PDI) batch and PDI at 12.5 and 200 µg ml ^{−1} (ref. 27)
Reactive oxygen species (ROS) and respective peak concentrations (µg ml ^{−1}) ²⁷

OECD Working Party on Manufactured Nanomaterials (WPMN)³⁰ (NM-400 – NM-403 & NRCWE-006 ‘a different batch of NM-400’). These MWCNTs were not functionalized and are called standard materials in the literature.²⁸ Additional samples were found in the literature, but due to incomplete information, they were not included in our analysis. The full list of available characteristics (features) of MWCNTs are presented in Table 1. The “Genotoxicity” endpoint was measured in both *in vivo* studies for DNA strand breaks (Comet assay) and *in vitro* studies in mammalian cells for gene mutation (micro nucleus).¹¹ Despite the different sources of the data, data integrity was secured since all studies were performed on the same MWCNTs.^{11,27,29}

The information available for each MWCNT was structured in a ready-for-modelling dataset including both physicochemical and toxicological information (Table S1 in the ESI†). The 15 MWCNTs with their partitioning into groups, the genotoxicity end-points and some key physicochemical features are presented in Table 2.

Data pre-processing

The data that were used in this study were mainly selected from three literature studies and are extensively presented in Table S1 of the ESI.†^{11,27,29} First step of the data pre-processing section was to fill the missing values of the physicochemical properties. In more details, “impurity” values, collected from the Poulsen *et al.* work,²⁹ contained percentages of impurities (wt%) in different metal oxides, resulting to a dataset with many missing values. In order to bypass this issue, a new feature was created (“Impurity”), as the summation of the different types of impurities. In addition, the “Endotoxins” values of NRCWE-041 and NM-400 analogues were missing, and were filled with the mean of the “Endotoxins” values of the rest of the materials in the same group.

Next step was the augmentation of the dataset. The standard deviations of “Diameter” values were used to create two new features: “Minimum Diameter” and “Maximum Diameter”.



Table 2 Overview of MWCNTs dataset. "Diameter" and "Length" were measured in nanometers (nm) representing the average values; "Endotoxins" in EU mg⁻¹, "BET" in m² g⁻¹ and "Impurity", "Purity" and "CEA" in percentages (%). "Impurity" was calculated as the percentage of total impurities. "Genotoxicity" was the binary endpoint indicating whether a MWCNT was considered as genotoxic (value "1") or non-genotoxic (value "0")

Group	Code	Type	Length	Diameter	BET	Impurity	Purity	CEA	Endotoxins	Genotoxicity
Group I	NRCWE-040	Pristine	518.9	22.1	150	0.773	98.60	96.00	0.18	0
	NRCWE-041	-OH	1005.0	26.9	152	0.462	99.20	97.00	0.22	0
	NRCWE-042	-COOH	723.2	30.2	141	0.321	99.20	96.00	0.26	0
Group II	NRCWE-043	Pristine	771.3	55.6	82	1.219	98.50	96.00	0.25	0
	NRCWE-044	-OH	1330.0	32.7	74	1.006	98.60	97.00	0.27	1
	NRCWE-045	-COOH	1553.0	30.2	119	2.782	96.30	93.00	0.34	1
Group III	NRCWE-046	Pristine	717.2	29.1	223	0.783	98.70	96.00	0.19	0
	NRCWE-047	-OH	532.5	22.6	216	0.781	98.70	97.00	0.01	0
	NRCWE-048	-COOH	1604.0	17.9	185	0.721	98.80	96.00	0.03	0
Standard Materials	NRCWE-049	-NH	731.4	14.9	199	0.738	98.80	97.00	0.05	0
	NM-400	Pristine	847.0	11.0	254	0.368	90.00	88.00	0.24	1
	NM-401	Pristine	4048.0	67.0	18	0.065	99.19	98.00	0.42	0
	NM-402	Pristine	1372.0	11.0	226	1.313	92.97	92.00	0.01	1
	NM-403	Pristine	1373.0	13.0	227	5.313	90.00	97.00	0.01	1
	NRCWE-006	Pristine	5700.0	65.0	26	0.680	99.00	98.00	0.51	1

Feature "Type" indicates the type of the functional group of an observation and was originally a categorical field. This feature was encoded *via* the "One-Hot Encode" method resulting to 4 new binary features: "Type_Pristine", "Type_OH", "Type_COOH" and "Type_NH2". For each analogue, these columns contained the value "0", except from the column that represented the specific type of the analogue, *e.g.* for analogue NRCWE-041 "Type_Pristine", "Type_COOH" and "Type_NH2" values were "0", whereas the "Type_OH" column had the value "1". The original "Type" column was then discarded.

The endpoint "genotoxicity" of this study was a binary column with values "1", indicating an analogue as genotoxic, and "0" indicating an analogue as non-genotoxic. The endpoint values were taken from the Aschberger *et al.* study.¹¹ Hence, according to the results of the *in vitro* chromosome aberration (micronucleus) analogues, NM-400, NM-402, NM-403 and NRCWE-006 were considered as toxic. In addition, results of *in vivo* DNA damage-comet assay indicated that NRCWE-044 and NRCWE-045 in different concentrations could result to DNA strand breaks, and these NMs were also considered as genotoxic.¹¹

Finally, all features were scaled between values "0" and "1" (Table S2†). Scaling was performed by subtracting from each feature the lowest value and dividing it with the difference between highest and lowest values (min-max scaling).

Train-Test Split

Instead of a random split, we preferred to use the Kennard-Stone (KS) algorithm³¹ for partitioning the available dataset into training and test sets. The KS method provides a uniform coverage over the available data and selects analogues for the training set, which are on the boundaries of the data set, so that the produced models cover a wide DOA²³ in the multi-dimensional input space. The basic idea behind the KS algorithm is that Euclidean inter-sample distances are calculated first and the most separated analogues, are selected as training data points.

Machine learning/chemoinformatics methodologies

In this study we used several supervised and unsupervised chemoinformatic techniques, in order to develop the most efficient model for predicting genotoxicity of MWCNTs. These techniques were applied using python 3.6.7.³²

Unsupervised techniques

Principal Component Analysis (PCA)^{33,34} is a technique that reduces dimensionality of the dataset and removes the noise and the redundant information. PCA produces an orthogonal transformation on a set of features (in this case MWCNTs' physicochemical properties) and creates new latent features, known as Principal Components (PCs). Each principal component is a linear combination of all primary features. PCs are orthogonal to each other.³⁵

Supervised techniques

Random Forest (RF)^{34,36} combines simple tree predictors in a way that each tree depends on the values of a random vector



sampled independently, while for all trees in the forest, the same distribution is applied. The RF model decides according to the leveraged Gini impurity of each tree (mean decrease in Gini) leading to predictive models that do not overfit during the training process.

Support Vector Machines (SVM)^{34,37} is a method that aims to represent the data as points in the multi-dimensional space, mapped in a way that the samples of each class are divided by the widest possible gap. Given a training set, SVM constructs a set of hyperplanes that discern the analogues according to their class (in this case genotoxic or non-genotoxic). Finally, the hyperplane with the largest distance to the nearest training sample of any class is chosen for the classification.

Logistic Regression (LR)^{34,38} is a statistical model that uses the “logistic function” in order to predict if a sample is labeled in class “0” or in class “1”. In LR, the logit function (log-odds) is calculated as a linear combination of the features and the values of this function can vary between 0 and 1. Then, by applying the logistic function the log-odds are converted to probability of class and also vary between 0 and 1. Finally, if the probability of a sample is higher than 0.5 the sample is labeled in class “1”, else it is tagged in class “0”.³⁹

Naive Bayes (NB)^{34,39} is a probabilistic model, based on the Bayes’ theorem (eqn (1)), assuming independence among the features. A Gaussian NB model (GNB) is a Naive Bayes model where the likelihood of the features is assumed to follow a Gaussian distribution (eqn (2)).

$$P(x_i|y) = \frac{P(x_i)P(y|x_i)}{P(y)} \quad (1)$$

$$P(x_i|y) = \frac{1}{\sqrt{2\pi\sigma_y^2}} \exp\left(-\frac{(x_i - \mu_y)^2}{2\sigma_y^2}\right) \quad (2)$$

Bayesian optimization

Bayesian optimization⁴⁰ is a technique that aims to minimize a function, $f(x)$ on a bounded set S . In Bayesian optimization, the basic idea is to construct a probabilistic model for $f(x)$ and use this model to decide the next point in S where the function will be evaluated. The Bayesian optimization method was applied for tuning the hyperparameters of the RF, LR and SVM methods. Table 3 presents the hyperparameters involved in the RF, SVM and LR methods, that were tuned during the training process.

Recursive feature elimination (RFE)

Recursive Feature Elimination (RFE)⁴¹ is a feature selection method. RFE removes iteratively the features with the lowest predictive importance until the specified number of features is reached. In order to apply this method, the machine learning algorithm should provide weights of the feature in the decision function of the produced model. In our analysis, the RFE method was applied to the RF³⁶ and LR algorithms.³⁸

Leverage method for defining DOA

DOA²³ is the physicochemical space on which the developed model is trained. Predictions on outliers (*i.e.* MWCNTs which are not inside the DOA) are not considered as reliable. DOA was defined, in this study, according to the Leverage method, which calculates a threshold depending on the number of features and the number of the training samples (eqn (3)). In the process of making prediction for a new MWCNT, the leverage value is calculated according to eqn (4), where X is the information matrix of the training set and x_i is the vector containing the input features of the new MWCNT.⁴² Query MWCNTs with leverage higher than the defined threshold are considered to be unreliably predicted.

$$\text{Threshold} = 3 \times \frac{(\text{number of features})}{(\text{number of training samples})} \quad (3)$$

$$h_i = x_i^T (X^T X)^{-1} x_i \quad (4)$$

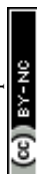
Results and discussion

In this study we developed two alternative workflows in order to select the most accurate and robust model for prediction genotoxicity of MWCNTs. The first workflow starts with the application of the PCA method, which reduces the dimension of the input space, by producing the principle components (PCs) or latent variables. The produced model still needs all the input features to calculate a prediction for a new MWCNT.

In the second workflow, the aim was to eliminate the “noisy” features, *i.e.* features which were not highly informative for predicting the endpoint of interest. The RFE method was used for selecting the most important variables.

Table 3 Hyperparameters that were tuned by the Bayesian optimization method

Model	Hyperparameter	Description
RF	n_estimators	Number of trees in the forest
	Min_samples_split	Minimum number of observations required to split a node
	Max_features	Maximum number of features to consider when looking for the best split of a node
LR	C	Inverse of regularization strength
	Penalty	Norm used in the penalization
SVM	C	Regularization parameter
	Gamma	Kernel coefficient
	Kernel	Kernel type



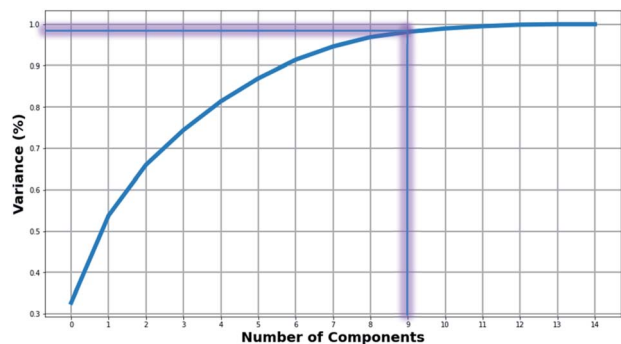


Fig. 2 Diagram representing the percentage of the explained variance as a function of the principal components.

Predictive modelling using the reduced dataset produced by PCA

Fig. 2 presents the level of variance explained by applying the PCA method as a function of the number of PCs. Two PCs explained slightly more than 65% of the variance. In order to maintain most of the available information, we proceeded with using the first nine PCs corresponding to explaining 96% of the variance (Table S3†).

For the selection of the testing samples, the KS algorithm³¹ was applied on the reduced dataset produced by the application of the PCA method. The following five analogues:

- NRCWE-040
- NRCWE-041
- NRCWE-048
- NM-401
- NM-402

were included in the test set, while the remaining 10 MWCNTs formulated the training set.

The RF, LR, SVM and NB statistical models were applied on the training set, in order to examine if the dimensional reduction process improves the prediction of genotoxicity endpoint. The hyperparameters of the RF, LR, SVM methods were optimized using the Bayesian optimization technique where the cross-validated accuracy score in the training set was the objective function that was minimised.⁴⁰ The optimal parameters are presented in Table 4.

The metrics of the models on the training set showed that all models were able to learn the underlying patterns of the

Table 4 The optimal hyperparameter values that were extracted from the Bayesian optimization technique,⁴⁰ for the models that were trained on the reduced PCA-dataset

Model	Hyperparameter	Optimal values
RF	n_estimators	9
	Min_samples_split	0.1025
	Max_features	0.6983
LR	C	43.71
	Penalty	L2
SVM	C	4.37
	Gamma	—
	Kernel	Linear

Table 5 Validation metrics for the models that were trained on the reduced PCA-dataset

	RF	LR	SVM	NB
Accuracy	0.800	0.800	0.800	0.600
Precision	0.000	0.50	0.500	0.000
Sensitivity	0.000	1.000	1.000	0.000
Specificity	1.000	0.750	0.750	0.750
F1-score	0.000	0.670	0.667	0.000
MCC	0.000	0.612	0.612	−0.250
Cross-validation	0.833	0.542	0.708	0.625
Confusion matrix	4	0	3	1
	1	0	0	1

training dataset, leading to an accuracy score of 1.0. The trained models were then used to predict the genotoxicity endpoint of the testing analogues. The performance of the produced models on the test set was examined using several classification metrics: confusion matrix, accuracy score, precision, specificity, sensitivity, F1-score and MCC metrics (eqn (S1)–(S7) of the ESI†). The accuracy score in a 4-fold cross validation test²⁵ was used to evaluate the robustness of the models. The results are summarized in Table 5.

The values of the metrics indicated that NB was unable to predict correctly two out of five testing samples. In addition, the RF model classified all the testing samples as non-genotoxic indicating a possible overfit of the model. The rest of the models had an accuracy score of 0.8 due to a misclassification of a non-genotoxic MWCNT. However, this particular MWCNT (NRCWE-048) is considered to be slightly out the domain of applicability of the models, hence it can be neglected. The low cross validation metric indicated that the LR and NB models failed the cross-validation test. The RF and SVM models' high cross-validation scores illustrated that both these models are highly robust.

Predictive modeling using feature selection

In our second approach the full dataset was considered first. The KS algorithm³¹ was used for splitting the *scaled-dataset* into training and testing subsets. The five selected testing analogues from this method were the same as in the PCA approach. The Bayesian optimization method⁴⁰ was applied on the training set for selecting the optimal values of the hyperparameters of the

Table 6 The optimal hyperparameter values that were extracted from the Bayesian optimization technique,⁴⁰ for the models that were trained on the full dataset

Model	Hyperparameter	Optimal values
RF	n_estimators	10
	Min_samples_split	0.5
	Max_features	0.1
LR	C	43.71
	Penalty	L2
SVM	C	9.98
	Gamma	0.254
	Kernel	Sigmoid



Table 7 Validation metrics for the models that were trained on the *full dataset*

	RF		LR		SVM		NB	
Accuracy	0.600		0.800		0.8000		0.600	
Precision	0.0333		0.500		0.333		0.333	
Sensitivity	1.000		1.000		1.000		0.500	
Specificity	0.500		0.500		0.750		0.500	
F1-score	0.500		0.667		0.500		0.500	
MCC	0.666		0.612		0.612		0.408	
Cross-validation	0.708		0.458		0.917		0.458	
Confusion matrix	2	2	3	1	3	1	2	2
	0	1	0	1	0	1	0	1

RF, LR and SVM methods using again the cross-validated accuracy metric as the objective function to be minimized. The optimal values are presented in Table 6.

The metrics of the models on the training set showed that all models were able to learn the training dataset. In more details, the RF, LR and NB models classified all training samples correctly, whereas the SVM model misclassified one non-genotoxic MWCNT, leading to a 0.9 training accuracy score and 0.82 MCC score. The produced models were validated on the *test-dataset* using the same classification metrics that were presented in the first approach. The results are presented in Table 7.

The performance of all produced models was clearly poorer compared to the models trained on the reduced PCA dataset. None of the models managed to predict correctly all the testing samples, while cross validation scores were lower, with the exception of the SVM method. The reason for this poor performance was the existence of noisy and non-informative features in the training set. Therefore, we proceeded with eliminating these variables, by applying the RFE method.⁴¹ This method was applied on the RF and LR algorithms only, because these models include attributes that distinguish the most significant features. The significances of the features in the LR model are represented by their coefficient at the exponential of the decision function, whereas the significance of the features in the RF models is indicated by the Gini criterion.³⁶ The importance of the features in the two models is presented graphically in Fig. 3.

Table 8 Most significant features of the LR and RF models after the application of the RFE method

Features for the LR model	Features for the RF model
Zeta average at 12.5 $\mu\text{g ml}^{-1}$	Zeta average at 12.5 $\mu\text{g ml}^{-1}$
Length (average)	Length (average)
Polydispersity index (batch)	Purity (%)
Purity (%)	—

The RFE iterative process⁴¹ was applied to exclude the less important features, by eliminating the features with the smallest importance in each iteration. The result of this process was the development of LR and RF models, which use only four or three features accordingly, as shown in Table 8.

The “Purity” of MWCNTs as well as the “Zeta average” values at a 12.5 $\mu\text{g ml}^{-1}$ dose and the “Length” were considered as significant features for both models. The two models were further optimized by applying the Bayesian optimization method. The optimal values of the hyperparameters are displayed in Table 9.

The performance of these trained models was tested by classifying both the training and the corresponding testing analogues. Both models classified correctly all training samples, leading to an accuracy score equal to 1.0. The metric values corresponding to the test set are presented in Table 10.

The accuracy score, precision, recall and F1-metrics and the confusion matrices all indicated that both LR and RF models were able to classify correctly the majority of the testing

Table 9 The optimal hyperparameter values that were extracted from the Bayesian optimization method,⁴⁰ for the LR and RF models that were trained on the four most significant features

Model	Hyperparameter	Optimal values
LR	C	4.37
	Penalty	L2
RF	n_estimators	19
	Min_samples_split	0.116
	Max_features	0.666

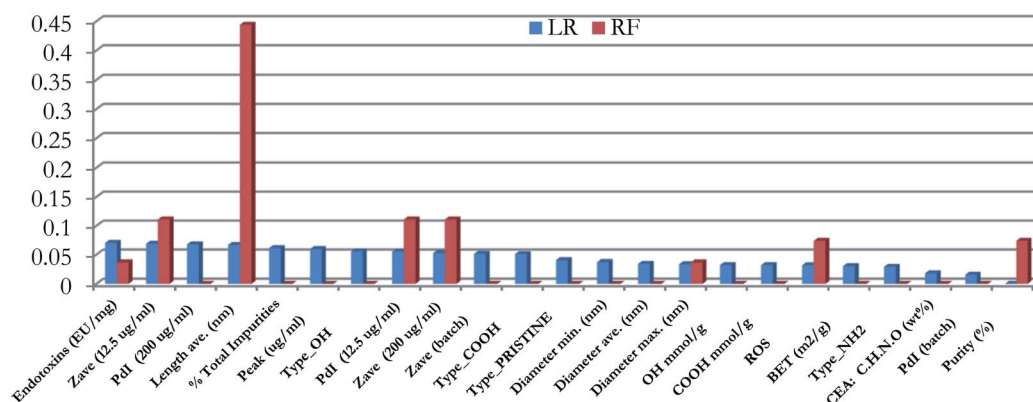
**Fig. 3** Scaled significance of features in the LR and RF models.

Table 10 Validation metrics for the models that were trained on the most significant features

	RF		LR	
Accuracy	0.800		0.800	
Precision	0.500		0.500	
Sensitivity	1.000		1.000	
Specificity	0.750		0.750	
F1-score	0.666		0.666	
MCC	0.612		0.612	
Cross-validation	0.917		1.000	
Confusion matrix	3	1	3	1
	0	1	0	1

samples. Among the two methods, LR had a higher cross-validation score and was more robust. To further evaluate the performance of the two models, we present in Table 11 the probability distributions of all predicted outputs over the set of two classes. The probabilities were similar for the RF and the LR models and not close to 0.5, which indicating that the successful classifications are not due to chance correlations.

Next step of the workflow was the calculation of DOA^{23,42} according to the Leverage method for the models. The thresholds were estimated to be equal to 1.2 for the LR model and 0.9 for the RF model and the values of the testing analogues are displayed below in Table 12. According to this table, all test MWCNTs were clearly within the DOA of the model, which further supported our confidence on the predictions of the model.

Final results and model selection

In the first workflow, the application of the PCA data reduction and transformation method affected positively the performance

Table 11 Classification probabilities of the RF and LR models after applying the RFE method,⁴¹ for the testing samples

MWCNT	RF		LR	
	Prob. of "0" class	Prob. of "1" class	Prob. of "0" class	Prob. of "1" class
NRWCE-040	0.74	0.26	0.74	0.26
NRWCE-041	0.74	0.26	0.82	0.18
NRWCE-048	0.68	0.32	0.73	0.27
NM-401	0.31	0.69	0.36	0.64
NM-402	0.00	1.00	0.31	0.69

Table 12 Leverage values of the testing samples

Name	RF		LR	
	Leverage value	Reliability	Leverage value	Reliability
NRCWE-040	0.20	Reliable	0.20	Reliable
NRCWE-041	0.18	Reliable	0.36	Reliable
NRCWE-048	0.33	Reliable	0.43	Reliable
NM-401	0.48	Reliable	0.51	Reliable
NM-402	0.13	Reliable	0.19	Reliable

of all models (increased precision and significantly improved the MCC metric). In the second workflow, the dimensional reduction of the dataset was achieved through the RFE method, which was applied on the RF and LR training procedures and resulted to models that use only 3 and 4 input features, accordingly, with 80% accuracy on the testing dataset. Several predictive models were produced as a result of the application of the two workflows. In order to select the best performing model, multiple criteria were taken into account:

(i) Prediction accuracy. High accuracy, sensitivity, specificity, recall, F1 and MCC scores on the external validation

(ii) Prediction confidence. Correct predictions with high probabilities

(iii) Robustness. High cross validation score

(iv) Simplicity. Use of a small set of input features

A number of models produced by the two workflows were highly successful with respect to the prediction accuracy criterion. The final LR and RF models were similar in terms of performance. The LR model's mean cross validation score is equal to 1.0 indicating that it may be considered as a slightly more robust model compared to the RF models (mean cross validation score 0.917). However, the simplicity criterion was considered as a key parameter to select the best model to classify the genotoxicity of MWCNTs. Under this consideration, the RF that predicted the genotoxicity end point using only three input features was selected as the model that outperformed the rest with respect to all other criteria: *highest cross validation score, high MCC score on the testing data, high probabilities of the predictions and use of only three features*. This model was chosen as the most efficient model for predicting genotoxicity of MWCNTs. The model was finally trained on the full dataset, in order to take into account all the information in the available dataset. The final model predicted correctly the genotoxicity endpoint for all samples in the full dataset. The threshold that defines the DOA of the full model was 0.9.

Web implementation of the model

The source code for developing the model is available at: <https://github.com/ntua-unit-of-control-and-informatics/MWCNTs> <https://github.com/ntua-unit-of-control-and-informatics/SPIONs>. The model has been implemented as a web service in the Jaqpot 5 modelling platform (<https://app.jaqpot.org/>) and is available in the following URL: <https://app.jaqpot.org/model/THPwkjY80z7yaIFNAYJR> under the BIORIMA organisation. In the overview tab, more details about the model are presented including a Predictive Markup Language (PML) representation which contains the scaling coefficients and the logit function. For accessing the model, the interested user should first register in Jaqpot 5 and then become a member of the BIORIMA organisation by sending an e-mail to: hsarimv@central.ntua.gr.

Discussion and conclusions

The remarkable properties of MWCNTs and their potential use in a wide range of applications has led researchers to consider



nanotubes based on carbon as one of the potential materials that may play key roles in the future of nanoscale-based applications. In this paper we have focused on developing a fully validated mathematical model for the prediction of genotoxicity of MWCNTs. Genotoxicity was selected as the toxicological endpoint, due to data completeness in literature and its relevance in risk assessment; it is a REACH requirement at the lowest tonnage level.²² Toxicological data of MWCNTs were extracted from both *in vivo* and *in vitro* studies.¹¹ The goal was to develop the most efficient classification model for MWCNTs (geno)toxicity by designing and executing two different cheminformatics workflows employing various state-of-the-art machine learning applications. After a thorough validation of the models using multiple performance criteria, a model produced by the RF method and the RFE variable selection procedure, was selected as the model with the best performance. Another efficient model using four descriptors only, was produced by the LR method. The “percentage of pure carbon”, the “Zeta average” and the “Length” play a significant role in the prediction for both models. The LR model selected an additional physicochemical characteristic (“the polydispersity index”). These results are in agreement with the literature. “Carbon purity” and “zeta potential” have been reported by Aschberger *et al.*¹¹ as important factors affecting MWCNTs genotoxic hazard potential. “Length” has also been suggested in the literature¹¹ as a critical factor for MWCNTs *in vivo* toxicity. More specifically, long MWCNTs were usually considered to be more hazardous⁴³ than short ones, in *in vivo* tests, causing cell death and ROS generation.^{44,45}

In conclusion, this study exhibited the value of using chemoinformatic techniques to produce a reliable model for predicting genotoxicity of MWCNTs. In future studies the predictive power of the model can be improved by considering information and data on extrinsic properties of the surrounding medium (pH, serum proteins, ionic strength).^{46,47}

Conflicts of interest

There are no conflicts to declare.

Acknowledgements

H. Sarimveis, C. Charitidis and M. Kotzabasaki acknowledge financial support by BIORIMA (Grant Agreement 760928), a project funded by the European Commission under the Horizon 2020 Programme.

Notes and references

- 1 R. Vajtai, *Springer Handbook of Nanomaterials*, 2013.
- 2 S. Iijima, *Nature*, 1991, **354**, 56–58.
- 3 W. Krätschmer, L. D. Lamb, K. Fostiropoulos and D. R. Huffman, *Nature*, 1990, **347**, 354–358.
- 4 S. Iijima and T. Ichihashi, *Nature*, 1993, **363**, 603–605.
- 5 N. Saifuddin, A. Z. Raziah and A. R. Junizah, *J. Chem.*, 2013, 676815.
- 6 C. Liu and H. M. Cheng, *Mater. Today*, 2013, **16**, 19–28.
- 7 M. F. Yu, B. S. Files, S. Arepalli and R. S. Ruoff, *Phys. Rev. Lett.*, 2000, **84**, 5552–5555.
- 8 A. Venkataraman, E. V. Amadi, Y. Chen and C. Papadopoulos, *Nanoscale Res. Lett.*, 2019, **14**(1), 220.
- 9 P. Sharma, N. Kumar Mehra, K. Jain and N. K. Jain, *Curr. Drug Delivery*, 2016, **13**, 796–817.
- 10 Y. Morimoto, M. Horie, N. Kobayashi, N. Shinohara and M. Shimada, *Acc. Chem. Res.*, 2013, **46**, 770–781.
- 11 K. Aschberger, D. Asturiol, L. Lamon, A. Richarz, K. Gerloff and A. Worth, *Comput. Toxicol.*, 2019, **9**, 22–35.
- 12 C. A. Poland, R. Duffin, I. Kinloch, A. Maynard, W. A. H. Wallace, A. Seaton, V. Stone, S. Brown, W. MacNee and K. Donaldson, *Nat. Nanotechnol.*, 2008, **3**, 423–428.
- 13 C. W. Lam, J. T. James, R. McCluskey and R. L. Hunter, *Toxicol. Sci.*, 2004, **77**, 126–134.
- 14 D. B. Warheit, B. R. Laurence, K. L. Reed, D. H. Roach, G. A. M. Reynolds and T. R. Webb, *Toxicol. Sci.*, 2004, **77**, 117–125.
- 15 N. Kobayashi, M. Naya, K. Mizuno, K. Yamamoto, M. Ema and J. Nakanishi, *Inhalation Toxicol.*, 2011, **23**, 814–828.
- 16 European Parliament, Council, Regulation (EC) No 1223/2009 of the European Parliament and of the Council of 30 November 2009 on cosmetic products, *Off. J. Eur. Union.*, 2009, **L342**, 59–209.
- 17 L. Lamon, K. Aschberger, D. Asturiol, A. Richarz and A. Worth, *Nanotoxicology*, 2019, **13**, 100–118.
- 18 S. C. Peter, J. K. Dhanjal, V. Malik, N. Radhakrishnan, M. Jayakanthan and D. Sundar, *Encyclopedia of Bioinformatics and Computational Biology*, 2019, vol. 2, pp. 661–676.
- 19 European Chemicals Agency, *Version 1.0*, 2017, pp. 1–29.
- 20 M. I. Kotzabasaki, I. Sotiropoulos and H. Sarimveis, *RSC Adv.*, 2020, **10**, 5385–5391.
- 21 T. X. Trinh, J.-S. Choi, H. Jeon, H.-G. Byun, T.-H. Yoon and J. Kim, *Chem. Res. Toxicol.*, 2018, **31**(3), 183–190.
- 22 European Parliament and Council, Regulation (EC) No 1907/2006 of the European Parliament and of the Council of 18 December 2006 REACH, *Off. J. Eur. Union.*, 2006, **L396**, 3–280.
- 23 K. Roy, S. Kar and P. Ambure, *Chemom. Intell. Lab. Syst.*, 2015, **145**, 22–29.
- 24 H. Abdi and L. J. Williams, *Wiley Interdiscip. Rev.: Comput. Stat.*, 2010, **2**, 433–459.
- 25 T. Hastie, R. Tibshirani, J. Friedman and J. Franklin, *Math. Intell.*, 2004, **27**(2), 83–85.
- 26 T. Kato, Y. Totsuka, K. Ishino, Y. Matsumoto, Y. Tada, D. Nakae, S. Goto, S. Masuda, S. Ogo, M. Kawanishi, T. Yagi, T. Matsuda, M. Watanabe and K. Wakabayashi, *Nanotoxicology*, 2013, **7**(4), 452–461.
- 27 P. Jackson, K. Kling, K. Jensen, P. Clausen, A. Madsen, H. Wallin and U. Vogel, *Environ. Mol. Mutagen.*, 2015, **56**(2), 183–203.
- 28 S. Poulsen, P. Jackson, K. Kling, K. Knudsen, V. Skaug, Z. Kyjovska, B. Thomsen, P. Clausen, R. Atluri, T. Berthing, S. Bengtson, H. Wolff, K. Jensen, H. Wallin and U. Vogel, *Nanotoxicology*, 2016, **10**, 1–39.



- 29 S. Poulsen, K. Knudsen, P. Jackson, I. Weydahl, A. Saber, H. Wallin and U. Vogel, *PLoS One*, 2017, **12**(4), e0174167.
- 30 K. Rasmussen, J. Mast, T. P. D. E. Verleysen, N. Waegeneers, F. Steen, J. Pizzolon, L. Temmerman, D. E. Van K. Jensen, R. Birkedal, P. Clausen, Y. Kembouche, N. Thieriet, O. Spalla, C. Guiot, D. Rousset, O. Witschger, S. Bau and C. Gaillard, *Multi-walled Carbon Nanotubes, NM-400, NM-401, NM-402, NM-403: Characterization and Physico-Chemical Properties*, Publications Office of the European Union, Luxembourg, 2014.
- 31 R. Kennard and L. Stone, *Technometrics*, 1969, **11**, 137–148.
- 32 G. V. Rossum and F. L. Drake, *Python Reference Manual, PythonLabs, Virginia USA*, 2001, <http://www.python.org>.
- 33 P. F. Karl, *London, Edinburgh Dublin Philos. Mag. J. Sci.*, 1901, **2**(11), 559–572.
- 34 F. Pedregosa, G. Varoquaux, A. Gramfort, V. Michel, B. Thirion, O. Grisel, M. Blondel, P. Prettenhofer, R. Weiss, V. Dubourg, J. Vanderplas, A. Passos, D. Cournapeau, M. Brucher, M. Perrot, E. Duchesnay and G. Louppe, *J. Mach. Learn. Res.*, 2012, 2825–2830.
- 35 I. Jolliffe and J. Cadima, *Philos. Trans. R. Soc., A*, 2016, **374**, 20150202.
- 36 L. Breiman, *Mach. Learn.*, 2001, **45**, 5–32.
- 37 B. Boser, I. Guyon and V. Vapnik, *Proceedings of the Fifth Annual ACM Workshop on Computational Learning Theory*, 1996, pp. 144–152.
- 38 J. Cramer, *SSRN Electron. J.*, 2002, 167–178.
- 39 H. Zhang, *Proceedings of the Seventeenth International Florida Artificial Intelligence Research Society Conference*, 2004, vol. 2.
- 40 B. Betrò, *J. Glob. Optim.*, 1991, **1**(1), 1–14.
- 41 B. Darst, K. Malecki and C. Engelman, *BMC Genet.*, 2018, **19**, 65.
- 42 F. Sahigara, M. Kamel, D. Ballabio, A. Mauri, V. Consonni and R. Todeschini, *Molecules*, 2012, **17**, 4791–4810.
- 43 F. Murphy, C. Poland, R. Duffin and K. Donaldson, *Nanotoxicology*, 2013, **7**(6), 1157–1167.
- 44 H. Johnston, G. Hutchison, F. Christensen, S. Read, S. Hankin, K. Aschberger and V. Stone, *Nanotoxicology*, 2010, **4**, 207–246.
- 45 G. Vietti, D. Lison and S. van den Brule, *Part. Fibre Toxicol.*, 2016, **13**, 11.
- 46 J. Arts, M. Irfan, A. Keene, R. Kreiling, D. Lyon, M. Maier, K. Michel, N. Neubauer, T. Petry, U. Sauer, D. Warheit, K. Wiench, W. Wohlleben and R. Landsiedel, *Regul. Toxicol. Pharmacol.*, 2016, **76**, 234–261.
- 47 A. Oomen, P. Bos, T. Fernandes, H. Kerstin, D. Borschi, H. Byrne, K. Aschberger, S. Gottardo, d. K. F. v. D. Kühnel, D. Hristozov, A. Marcomini, L. Migliore, J. Scott-Fordsmand, P. Wick and R. Landsiedel, *Nanotoxicology*, 2014, **8**(3), 334–348.

